Carbohydrate Polymers 121 (2015) 284–294

Contents lists available at ScienceDirect

Carbohydrate Polymers

journal homepage: www.elsevier.com/locate/carbpol

Effects of the addition of dimer acid alkyl esters on the properties of ethyl cellulose

Sangjun Lee[a,b], Kwang-Hwan Ko[c], Jihoon Shin[a], Nam-Kyun Kim[a], Young-Wun Kim[a,b,*], Joon-Seop Kim[c,*]

[a] White Biotechnology Research Group, Korea Research Institute of Chemical Technology, 141 Gajeong-ro, Yuseong-gu, Daejeon 305-600, South Korea
[b] Department of Green Chemistry and Environmental Biotechnology, Korea University of Science & Technology, 113 Gwahak-ro, Yuseong-gu, Daejeon 305-600, South Korea
[c] Department of Polymer Science & Engineering, Chosun University, 309 Pilmun-daero, Dong-gu, Gwangju 501-759, South Korea

ARTICLE INFO

Article history:
Received 5 October 2014
Received in revised form
26 November 2014
Accepted 3 December 2014
Available online 31 December 2014

Keywords:
Plasticizer
Waste vegetable oil
Dimer acid esters
Ethyl cellulose

ABSTRACT

In this study, we synthesized dimer acid (DA) esters, having short to long alkyl chains, (DA-C_n) by the Diels–Alder reaction and subsequent esterification reaction of fatty acids that were prepared by the hydrolysis of waste vegetable oil. It was found that the DA-C_n were thermally more stable than common petroleum-based plasticizer DOP. When the DOP, DA, or DA-C_n with short alkyl chains were added to ethyl cellulose (EC), the optical clarity and SEM images of the samples showed their good miscibility with those additives in a micro-scale. It was also found that the rubbery modulus of the EC decreased with increasing amount of additives; the type of the additives did not affect the rates of the decrease in the rubbery modulus. The main transition temperatures of the EC containing either DA or DA-C_1 or DA-C_4 decreased with increasing amounts of those additives and were comparable to that of the DOP-containing EC. The above findings suggested that the DA and its esters with short alkyl chains could act as effective plasticizer and, thus, could be used instead of the DOP. In addition, the results obtained from tensile testing and leaching experiments implied that the DA might be better plasticizer than the DA-C_1 and DA-C_4, at least in some cases, because of hydrogen-bonding with the EC.

1. Introduction

In the 20th century, petroleum-based materials had become main row materials and chemicals in the field of material science and technology; however, eventually, they were recognized as a major cause of carbon dioxide emissions that is, now, widely blamed for global warming (Rem, Olsen, Welink, & Fraunholcz, 2009; Halden, 2010). In addition, the upsurge in oil prices due to the depletion of oil resources has also led us to the reduction of the use of petroleum-based fuel. Thus, many researchers continue and spur the development of materials from bio-based resources instead of petrochemical resources. Most of these eco-friendly bio-based materials made from renewable resources are bio-plastics and have the merits of solving the oil depletion problems and environmental pollution problems caused by plastics waste (Qin & Wang, 2010; Chen & Patel, 2012). The typical examples of the bio-plastics are poly(lactic acid) and poly(hydroxyalkanoate). However, the bio-plastics have the drawbacks of very high unit costs of production and deteriorating physical properties such as poor heat resistance (Lunt, 1998; Luckachan & Pillai, 2011). To overcome these shortcomings, many researchers have been actively studying composite materials that consist of relatively cheap, abundant and renewable natural polymers (e.g. cellulose, starch, chitosan, etc.) and inorganic filler.

Ethyl cellulose (EC) is one of cellulose derivatives, some of the hydroxyl groups of the glucose units of cellulose are converted into ethyl ether groups, and shows excellent mechanical properties, stability, and biocompatibility (Rekhi & Jambhekar, 1995; Gupta & Sahoo, 2001). However, the hydrogen bonds between the hydroxyl groups of the repeating units make the processing of the EC difficult, which limits its applications (Bodmeier & Paeratakul, 1994). In plastics industry, phthalate plasticizers (e.g. di(2-ethylhexyl)phthalate (DOP) and diisodecyl phthalate) have been applied to weaken the intermolecular interactions and enhance the mobility of polymer

* Corresponding authors at: White Biotechnology Research Group, Korea Research Institute of Chemical Technology, 141 Gajeong-ro, Yuseong-gu, Daejeon 305-600, South Korea and Department of Polymer Science & Engineering, Chosun University, 309 Pilmun-daero, Dong-gu, Gwangju 501-759, South Korea.
Tel.: +82 42 860 7605/+82 62 230 7211; fax: +82 42 860 7669/+82 62 232 2474.
E-mail addresses: ywkim@krict.re.kr (Y.-W. Kim), joon@chosun.ac.kr (J.-S. Kim).

http://dx.doi.org/10.1016/j.carbpol.2014.12.029
0144-8617/

chains, which leads to the easier processing of brittle polymer such as EC (Rahman & Brazel, 2004). Recently, however, it has been reported that some of the phthalates are endocrine disruptors and toxic. In addition, sometimes external plasticizers leach out of plastics in a certain period of time. Thus, in some countries the use of some of phthalates as external plasticizers has been strictly restricted for use in medical plastics, toys for children and child care items (Peña, Hidalgo, & Mijangos, 2000; Krauskopf, 2003), which urges the development of eco-friendly plasticizer (Labrecque, Kumar, Davé, Gross, & McCarthy, 1997). In this case, the eco-friendly plasticizer should meet the strict requirements in terms of better biocompatibility, biodegradability, and renewability, compared to petroleum-based plasticizer (Rahman & Brazel, 2004).

Dimer acid (DA), a yellow viscous liquid at room temperature, is renewable materials that can be synthesized by dimerization of fatty acids obtained from vegetable oils. The DA has non-crystallinity, high molecular weights and more than two reactive functional groups, and thus, the useful applications of the DA have been as oil additives, lubricants, and materials used in the preparation of resins, hot-melt adhesives, surfactants, inks or coatings (Fan, Deng, Waterhouse, & Pfromm, 1998). Furthermore, bio-based and non-toxic properties of DA allow its usage as eco-friendly materials. Thus, in the present work, we attempted to study DA and its ester forms that can be used as the eco-friendly plasticizer for the EC. Thus, we synthesized DA, using waste soybean oil as a raw material, and dimer acid derivatives, i.e. dimer acid alkyl ester (DA-C_n, here n = the number of carbon atoms of alkyl group), and characterized them, and prepared the EC materials containing DA or DA-C_n. Then, the thermal and mechanical properties and leachability of the EC materials were investigated.

2. Experimental

2.1. Materials

The reagents such as ethyl cellulose, di(2-ethylhexyl)phthalate (99%), methanol (anhydrous, >99.8%), 1-butanol (anhydrous, 99.8%), 2-ethylhexan-1-ol (>99%), and *p*-toluenesulfonic acid monohydrate (>99%) were purchased from Sigma-Aldrich. Isotridecanol (>99%) was purchased from Sasol. Toluene (HPLC grade) and chloroform (HPLC grade) were obtained from Samchun. The reagents and solvents were used without further purification. The number-average molecular weight (M_n = 20,000) and molecular weight distribution (MWD = 2.22) of ethyl cellulose (viscosity 4 cP, 5% in toluene/ethanol 8/2 (v/v)) were determined at 35 °C using an Agilent 1260 LC system with one PLgel guard column (5 μm, 50 × 7.5 mm) and three PLgel Mixed-C columns (5 μm, 300 × 7.5 mm) connected in series with $CHCl_3$ as the solvent (flow rate of the eluent = 1 mL/min). Shodex SM-105 polystyrene standards were used for alibration of the columns. The degree of substitution (*DS*) of EC sample (2.45–2.57) was calculated using the ethoxyl labeling (48–49.5%) given by the manufacturer as follows:

$$DS = \frac{(\text{ethoxyl content} \times (246.3 - 29.1 \times 3))}{(45.1 - \text{ethoxyl content} \times 29.1)} \quad (1)$$

here 246.3 = molecular weight (M_W) of fully substituted ethyl cellulose unit, 45.1 = M_W of ethoxyl group, 29.1 = M_W of ethyl group.

2.2. Characterization methods

The ^1H- and ^{13}C-nuclear magnetic resonance (NMR) spectra of the compounds dissolved in $CDCl_3$ were obtained using a Bruker DPX-300 spectrometer (300 MHz and 75 MHz, respectively). Tetramethylsilane was used as the internal standard. The Fourier transform infrared (FT-IR) transmittance spectra of the compounds were acquired in the range of 4000 to 550 cm^{-1} using a Bio-RAD FTS165 spectrometer. For the gas chromatography–mass spectrometry (GC/MS) study to determine the composition of fatty acids (FAs), an Agilent Technologies 7890 A GC/MS instrument, equipped with electron ionization and HP-1 capillary GC column (30 m (length) × 0.25 mm (inner diameter)) was used. A temperature range was 50–320 °C, a heating rate was 10 °C/min, a split ratio was 1:50, and injector and detector temperatures were ca. 250 and 300 °C, respectively. The molar mass and composition of FAs were also determined using size exclusion chromatograph at 40 °C using three Styragel columns (i.e. two HR 0.5 (7.8 × 300 mm) columns and one HR 1.0 (7.8 × 300 mm) column) connected in a series, with tetrahydrofuran as the solvent. Six of polyglycerol fatty acid ester standards (molecular weight = 280, 360, 620, 880, 1200, and 1500) were used for the calibration of the columns. The high-performance liquid chromatography (Waters HPLC system) for the quantitative analysis of the DA and DA-C_n derivatives were also carried out. The total acid number (TAN) of the compounds was determined by a base titration technique (ASTM D664) using a Metrohm 888 Titrando titrator.

2.3. Synthesis of DA-C_n

As shown in Scheme 1, dimer acid (DA) (85%) containing a small amount of trimer acid (TA) (15%) were synthesized by the hydrolysis and subsequent Diels–Alder reaction of fatty acids (FAs). Then, DA and TA ester derivatives were prepared by the esterification between corresponding the DA and TA, respectively, and proper alcohols.

2.3.1. Preparation of DA

FAs were prepared by the hydrolysis of waste soybean oil at 180–200 °C. The chemical composition of the FAs analyzed by GC/MS is C16:0 (4.7%), C16:1 (0.8%), C18:0 (0.7%), C18:1*c* (37.0%), C18:2*c* (50.4%), C18:3 (6.2%), others (balance); here, the number right next to capital "C" indicates the number of carbon atoms of the molecule, and the number right next to colon indicates the number of double bonds of the molecule, and "*c*" indicates *cis* isomer form. The preparation method, modified from the work by Paschke, Peterson, and Wheeler (1964) and Wheeler and White (Wheele & White, 1967), is described briefly here. For the preparation of the DA, the FAs (30 g), clay catalyst (2.4 g, 8 wt%), H_3PO_4 (0.026 g, 0.085 wt%), and deionized water (0.6 g, 2 wt%) were put in a high-pressure stainless-steel reactor equipped with a mechanical stirrer, a cooling water jacket, and a temperature controller. The reactor was sealed, evacuated for 30 min, and backfilled with N_2 four times to remove O_2 completely. The mixture in the reactor was heated to 250 °C and stirred for 12 h, and, then, cooled to room temperature and neutralized with H_3PO_4. After that, the mixture was heated again to 80 °C and stirred for 1 h. The mixture was cooled to room temperature and filtered to remove salts. The unreacted FAs in the filtrate were removed by vacuum distillation to obtain a product (27 g, yield = ca. 90%). HPLC analysis revealed that the product was composed of ca. 85 wt% of dimer acid and ca. 15 wt% of trimer acid. From now on, we use "DA" as a product notation instead of "the mixture of dimer acid (DA) and trimer acid (TA)" throughout the paper. At this point, it should be mentioned that the detailed studies on the effect of reaction conditions and source of fatty acids had already been conducted by our group and the findings have been reported elsewhere; interested readers are referred to the original article (Lee et al., 2013). For the sake of convenience, only brief results are given here. We found that the various waste vegetable oils, such as used soybean oil or by-products obtained in course of the production of edible oils, can be converted to fatty acids that can be used for synthesis of DA. Depending on oil sources, various fatty acids were obtained. With increasing the proportion of unsaturated fatty acids, overall yield percentages and the relative amount of TA were found

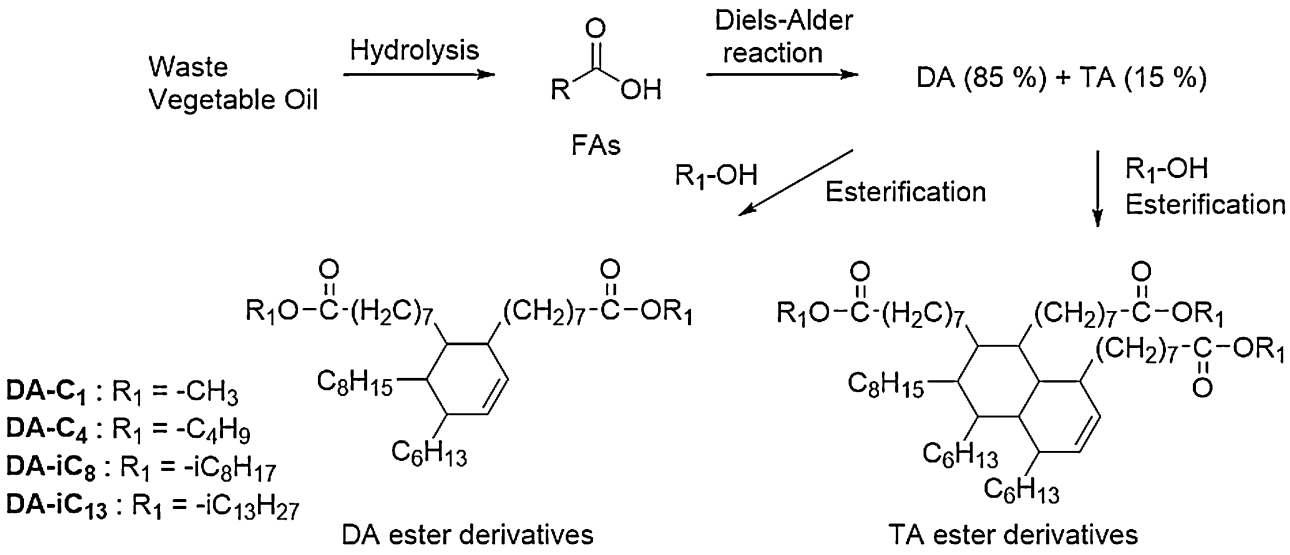

Scheme 1. Brief synthetic route of DA and TA and their ester derivatives.

to be increased. In addition, when the reaction time increased from 6 h to 24 h, the overall yield percentage increased from ca. 61% to ca. 90%. On the other hand, the relative amount of TA increased from ca. 10% to ca. 20%. Finally, we observed that the effect of the amount of catalyst was the same as that of the reaction time.

2.3.2. Preparation of DA-C_n

For the preparation of methyl ester of DA (DA-C_1), the DA (30 g, 53.5 mmol) and *p*-toluenesulfonic acid (0.92 g, 5.35 mmol) were placed in a 4-neck round-bottom flask equipped with a Dean–Stark apparatus and a condenser. The mixture in the flask was stirred at 150 °C, and methanol (5.14 g, 160 mmol) was added to the mixture slowly for 2 h to produce the DA-C_1. Then, the mixture was cooled to room temperature, neutralized with saturated $NaHCO_3$ solution, and finally washed with water three times. The product was dried using $MgSO_4$, and the residual solvent was evaporated to dryness to afford brownish oily product (30 g, yield = ca. 96%). Other DA-C_n esters were prepared using a similar method. The sample notations used here for the DA methyl ester, DA butyl ester, DA 2-ethylhexyl ester, and DA 11-methyldodecyl ester are DA-C_1, -C_4, -iC_8, and -iC_{13}, respectively.

2.4. Thermogravimetic analysis

For the thermogravimetric analysis (TGA) of DOP, DA, and DA-C_n derivatives, a TA Q-500 TGA instrument was used. The samples were heated from 25 °C to 600 °C at a heating rate of 10 °C/min under N_2 at a flow rate of 20 mL/min. The temperature for 5% weight loss ($T_{d\text{-}5\%}$) was determined.

2.5. Film preparation

To investigate the thermal properties of EC containing DA-C_n, we prepared the samples in a film form by using a solution casting method, described in literature (Tarvainen, Sutinen, Peltonen, Tiihonen, & Paronen, 2002); the amounts of the DA-C_n in the samples were 10, 20, 30, 40 and 50 phr. First of all, the EC and DA-C_n were dissolved in chloroform to make 5% (w/v) solutions. The solutions were then stirred for 3 h at room temperature. Then the solutions were poured into clean Teflon petri dishes (diameter = 10 cm), and the dishes were covered with their lids. The solutions were dried in an ambient condition for 1 week, which led to the film formation. Subsequently, the films were dried further under vacuum at 50 °C for another 1 week. The films were stored in a desiccator prior to use. The notations used for the EC containing either DOP or DA or DA-C_n are either EC-DOP(x) or EC-DA(x) or EC-DA-C_n(x), respectively; x indicates the amount of additives in the material in phr. A Philips XL30S FEG scanning electron microscope (SEM) was utilized to monitor the surface morphology of the films. To determine the optical clarity of the film samples (film thickness = 0.2 mm), the digital camera (Samsung NX-mini) was used to take photos of the film samples against the scene of our laboratory as a background. In addition, for the quantitative analysis of the film clarity, the UV–vis spectrophotometer (Shimadzu) was also used to determine the transmittance of the films exposed to the light (wavelength = 600 nm).

2.6. Mechanical property measurements

The dynamic mechanical properties of the EC samples were evaluated using a TA dynamic mechanical analyzer (DMA, Q-800) in a temperature sweep mode from 30 °C to 250 °C at 1 Hz. The heating rate was 1 °C/min. The specimens for the DMA in the form of a rectangular bar (30 mm × 7 mm × 2 mm) were prepared by compression molding of samples at 200–230 °C and under a pressure of 20 MPa for 5 min. The tensile strength (σ) and elongation (ε) of the sample were determined using an Instron 4482 testing machine with a 100 N load cell. The specimens in the form of a film for the tensile test (100 mm × 100 mm × 0.30 mm) were also prepared by compression molding at 160 °C and under a pressure of 7 MPa for 5 min, and the molded films were cut into strips (60 mm × 6 mm × 0.30 mm). The experimental condition was 25 °C and 50% relative humidity. The initial distance between the tensile grips and cross-head speed were 30 mm and 10 mm/s, respectively. The tensile strength was calculated as the maximum force at break divided by the cross-sectional area of the specimen, and the elongation at break was treated as the percentage of the length of specimen at break, compared to the initial length. An elastic modulus, i.e. Young's modulus, was calculated from the slope of the linear portion of the stress–strain curve in the elastic deformation region.

2.7. Leaching test

The measurement of the leachability of the DA or DA-C_n from the EC film samples was conducted using a modified version of ASTM D1239 for Resistance of Plastic Films to Extraction by Chemicals.

Deionized water was used as the extraction solvent, and the EC films containing DA or DA-C_n (50 mm × 50 mm × 0.20 mm) were also prepared by a casting method using chloroform as the solvent. For the leaching test, the film samples were immersed in deionized water for 24 h; the water container was placed in a chamber set to keep 23 ± 2 °C and 50 ± 5% relative humidity. Then, the films were fully dried in a vacuum oven at 50 °C for 1 week.

3. Results and discussion

3.1. Characterization of DA and DA-C_n esters

The TAN of the DA and DA-C_n are listed in Table 1.

First of all, it is clear that the TAN of the DA obtained by titration is almost the same as that (200.0 mg KOH/g) obtained by the calculation based on the chemical structures of dimer acid (85 wt%) and trimer acid (15 wt%). Second, zero or very small TANs of the DA-C_n indicate that the esterification of the DA is successfully complete.

The ^{1}H- and ^{13}C-NMR, and FT-IR spectra of the DA and DA-C_n were obtained to confirm their chemical structures. For the convenience of readers, only some of the ^{1}H NMR, ^{13}C-NMR and FT-IR spectra are discussed below. Figs. 1–3 show the ^{1}H- and ^{13}C-NMR, and FT-IR spectra of the FA, DA, and DA-C_n, respectively. In Fig. 1, one can find that, upon the Diels–Alder reaction of the FA, the NMR peaks for the olefinic protons of the FA at δ = 5.3 ppm and methylene protons between two double bonds of the FA at δ = 2.8 ppm disappear, and new peaks of low intensity, derived from cyclic olefinic protons, appear for the DA and DA-C_n at δ = 6.5–7.5 ppm. In addition, upon the esterification of the DA, new NMR peaks of the methyl protons of the DA-C_1 appear at δ = 3.65 ppm, and those of the methylene protons of the DA-C_4, DA-iC_8 and DA-iC_{13} are present at δ = 3.98 ppm. The positions of the ^{1}H NMR peaks of the DA and DA-C_n are also summarized in Table 1.

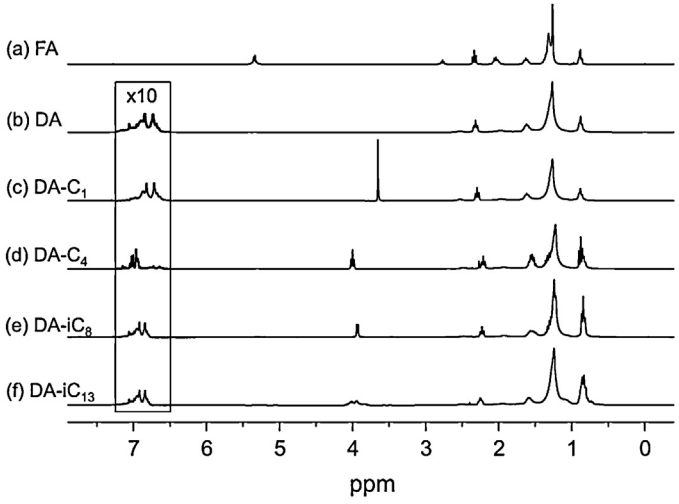

Fig. 1. ^{1}H NMR spectra of (a) FA, (b) DA, (c) DA-C_1, (d) DA-C_4, (e) DA-iC_8, and (f) DA-iC_{13}.

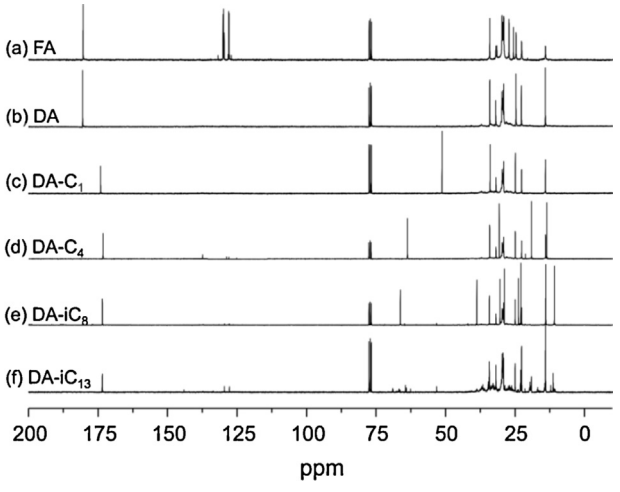

Fig. 2. ^{13}C NMR spectra of (a) FA, (b) DA, (c) DA-C_1, (d) DA-C_4, (e) DA-iC_8, and (f) DA-iC_{13}.

In Fig. 2, it is seen that the ^{13}C NMR spectrum of the DA is very similar to that of the FA, except for the absence of the NMR peaks for the olefinic protons of the FA at δ = 130 ppm. At this point, it should be mentioned that the NMR peaks for the cyclic unsaturated carbons are difficult to detect because of their low intensity. Upon the esterification, the NMR peak for the acid carbonyl group of the DA at δ = 180.6 ppm shifts to δ = 174.2 ppm for the ester carbonyl of the DA-C_1. The peak for the ester carbonyl of other DA-C_n with n = 4, 8, 13 appears in the range of δ = 173.3–173.6 ppm. The NMR peaks for the new terminal methyl carbons adjacent to the ester group of the DA-C_1 appear at δ = 51.3 ppm. In the case of other DA-C_n with n = 4, 8, 13, the peaks appear in the range of δ = 63.7–66.4 ppm. The positions of the ^{13}C NMR peaks of the DA and DA-C_n are also summarized in Table 1.

The FT-IR spectra of the FA, DA and DA-C_n are shown in Fig. 3. A typical strong IR band caused by the stretching mode of the acid carbonyl group of the FA and DA are shown at ν = 1710 cm^{-1}. This strong IR band is due to the cyclic dimerization of two carboxylic acid groups that can form hydrogen bonds. After the esterification reaction, the IR band for the carbonyl stretching of the DA-C_n shifts to ν = 1738–1743 cm^{-1}. Also, a broad IR band for O—H stretching is not shown at ν = 3083 cm^{-1} for the DA-C_n, whereas the spectra of the FA and DA show only the obscured O—H stretching band. The positions of the IR bands of the DA and DA-C_n are also summarized in Table 1.

3.2. Optical properties of EC containing DOP, DA, or DA-C_n

Fig. 4 shows the photographs of the EC, EC-DOP(30), EC-DA(30), EC-DA-C_1(30), EC-DA-iC_8(30), and EC-DA-iC_{13}(30) films against the scene of our laboratory as a background, and the SEM images of the surfaces of the films. From the photographs, one can find that the films of the EC, EC-DOP, EC-DA, EC-DA-C_1, and EC-DA-C_4 (not shown here) are relatively transparent, implying that the additives are miscible with the EC, at least in a micro-scale. On the other hand, the films of the EC-DA-iC_8 and EC-DA-iC_{13} are optically opaque.

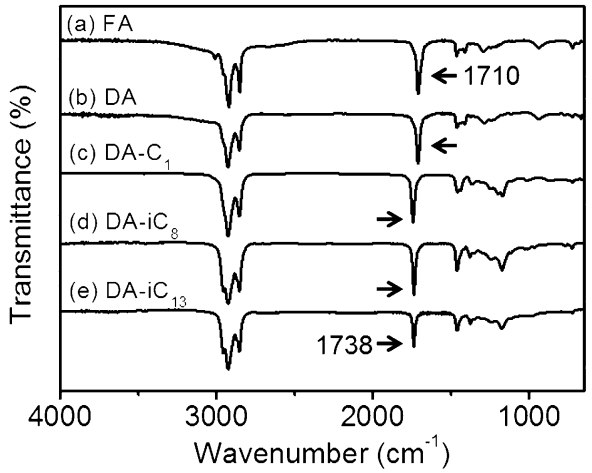

Fig. 3. FT-IR spectra of (a) FA, (b) DA, (c) DA-C_1, (d) DA-iC_8, and (e) DA-iC_{13}.

Table 1
TAN, NMR, IR, and $T_{d\text{-}5\%}$ data of DA and DA-C_n.

Compounds	TAN (mg KOH/g)	Positions of ^{1}H NMR peaks, δ (ppm)	Positions of ^{13}C NMR peaks, δ (ppm)	Positions of IR bands, ν (cm^{-1})	$T_{d\text{-}5\%}$ (°C)
DA	198.5	2.54 (m, 1*H*), 2.32 (t, 4*H*), 1.98 (m, 3*H*), 1.62 (m, 6*H*), 1.26 (m, 33*H*) 0.88 (t, 6*H*)	180.6, 34.1, 32.0, 29.8–29.1, 24.7, 22.8, 14.1	3083, 2925–2853, 1710, 1463, 1285, 937	294
DA-C_1	0.0	3.65 (s, 6*H*), 2.53 (m, 1.2*H*), 2.30 (t, 4.5*H*), 1.97 (m, 2.3*H*), 1.62 (m, 7*H*), 1.26 (m, 38.2*H*), 0.88 (m, 7*H*)	174.2, 51.3, 34.0, 31.9, 29.6–29.1, 24.9, 22.7, 14.1	2926–2854, 1743, 1461, 1363, 1171	284
DA-C_4	0.0	4.0 (t, 4*H*), 2.48 (m, 1*H*), 2.21 (t, 5.4*H*), 1.94 (m, 2*H*), 1.56 (m, 10.5*H*), 1.22 (m, 41*H*), 0.85–0.75 (m, 12*H*)	173.3, 63.7, 34.1, 31.9, 30.7, 29.6–29.1, 24.9, 22.6, 21.2, 19.1, 14.0, 13.6	2925–2851, 1736, 1460, 1356, 1177	267
DA-iC_8	0.042	3.98 (d, 4*H*), 2.51 (m, 1*H*), 2.25 (t, 4.2*H*), 1.95 (m, 2*H*), 1.59 (m, 8.4*H*), 1.25 (m, 53*H*), 0.85–0.75 (m, 19*H*)	173.6, 66.4, 38.8, 34.3, 31.9, 30.4, 29.6–28.9, 25.0, 23.8, 22.9, 22.6, 13.9, 10.9	2926–2855, 1738, 1463, 1379, 1174	273
DA-iC_{13}	0.006	3.98 (d, 4*H*), 2.49 (m, 1*H*), 2.28 (t, 4*H*), 1.97 (m, 2*H*), 1.58 (m, 2*H*), 1.24(65*H*), 0.88 (m, 27*H*)	173.5, 65.7, 38.2, 33.9, 32.1, 30.1, 29.9–28.4, 24.8, 23.7, 22.9, 22.6, 13.6, 10.8	2925–2855, 1738, 1462, 1378, 1176	271

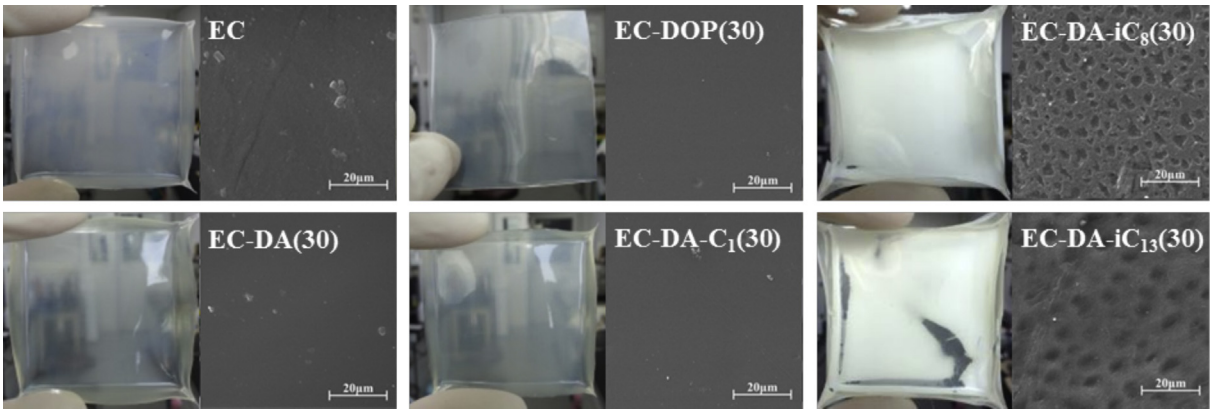

Fig. 4. Photographs of the EC films containing DOP, DA, DA-C_1, DA-iC_8, or DA-iC_{13} against the scene of our laboratory as a background and SEM images of the film surface.

The SEM images suggest that the surface of the EC, EC-DOP, EC-DA and EC-DA-C_1 films are smooth and uniform without micro-sized phase-separation, suggesting indirectly the relative transparency of the films. However, the SEM images of the EC-DA-iC_8 and EC-DA-iC_{13} films show micrometer-sized holes dispersed in the EC matrix randomly; this might result in the film opaqueness.

The optical clarity of some of the films was quantitatively measured by using UV–vis spectrophotometer. The results are listed in Table 2.

It is seen that the UV–vis transmittance of the EC-DOP, EC-DA and EC-DA-C_1 increases from ca. 56% to ca. 76–86% with increasing additive contents. This can be understood: If the DOP, DA, and DA-C_1 were miscible with the EC, the material could be homogeneous and relatively transparent. Then, with increasing amount of the additives the relative amount of the EC in the film decreases, which, in turn, leads to the dilution effect of the EC. If this were the case, it would be natural for the EC-DOP, EC-DA and EC-DA-C_1 to exhibit an enhanced UV–vis transmittance of the EC films; this might be what we observed here. However, the UV–vis transmittances of the EC-DA-iC_8 and EC-DA-iC_{13} are lower than that of the EC and remain constant at ca. 40%, which is due to the micro-sized phase-separation of the additives.

Table 2
UV–vis transmittance of EC, EC-DOP, EC-DA, and EC-DA-C_n.

Films	UV–vis transmittance (%)	Films	UV–vis transmittance (%)
EC	56.0	EC-DA-C_1(20)	63.7
EC-DOP(10)	60.2	EC-DA-C_1(30)	69.3
EC-DOP(30)	80.4	EC-DA-C_1(40)	73.6
EC-DOP(50)	85.6	EC-DA-C_1(50)	76.3
EC-DA(10)	50.0	EC-DA-iC_8(10)	39.5
EC-DA(20)	61.9	EC-DA-iC_8(20)	39.8
EC-DA(30)	70.7	EC-DA-iC_8 (30)	39.2
EC-DA(40)	77.2	EC-DA-iC_{13}(10)	40.4
EC-DA(50)	80.5	EC-DA-iC_{13} (20)	39.9
EC-DA-C_1(10)	50.1	EC-DA-iC_{13}(30)	39.2

To investigate the interactions between the hydroxyl groups of the EC and the carboxylic acid groups of the DA or the ester groups of the DA-C_n, we used an FT-IR technique. As seen in Fig. 5, the EC shows the IR bands for the hydroxyl groups and the ether groups at $\nu = 3475\,cm^{-1}$ and $\nu = 1050\,cm^{-1}$, respectively, but no IR band for the carbonyl groups at $\nu = 1710\,cm^{-1}$ because the EC does not have a carbonyl group. On one hand, as mentioned earlier, pure DA shows one strong IR band at $\nu = 1710\,cm^{-1}$ for the stretching mode of the carbonyl group of carboxylic acids that take part in the formation of hydrogen bonds between them. On the other hand, the EC-DA shows two IR bands for the stretching mode of the carbonyl group at $\nu = 1710$ and $1735\,cm^{-1}$, which will be discussed later. Pure DA-C_1 exhibits a strong IR band for the stretching mode of the carbonyl group of methyl ester at $\nu = 1743\,cm^{-1}$, but the EC-DA-C_1 exhibits only a weak IR band at the same wavenumber. This can be understood: the intensity of the IR band for the stretching mode of the carbonyl group should naturally be lower for the

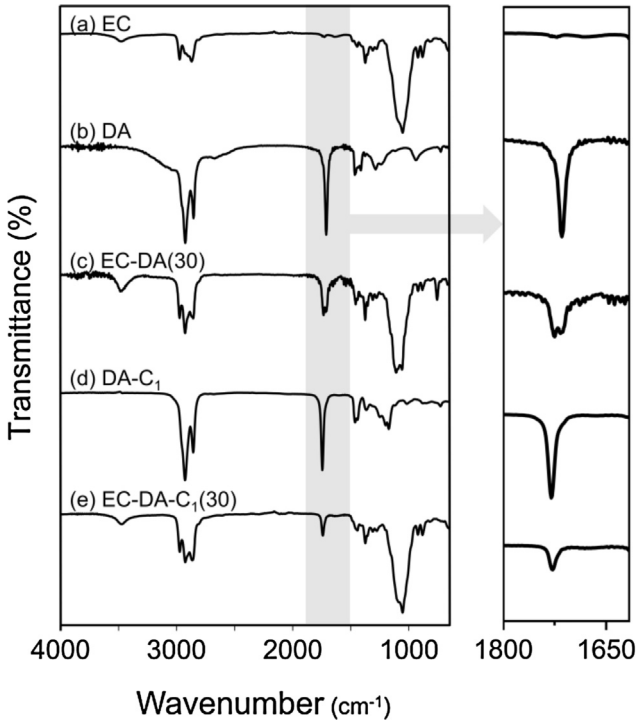

Fig. 5. FT-IR spectra of (a) EC, (b) DA, (c) EC-DA(30), (d) DA-C_1 and (e) EC-DA-C_1(30).

EC-DA-C_1, compared to that for the DA-C_1, because of a dilution effect. Now, let us discuss the two IR bands for the carbonyl groups of the EC-DA. The EC polymer chains contain a large amount of ether groups and a small amount of hydroxyl groups; the ether groups are poor proton acceptors (De Brabander, Van den Mooter, Vervaet, & Remon, 2002). This implies that there are two types of carbonyl groups in the EC-DA (Lizaso, Muñoz, & Santamaría, 1999). One is the carbonyl groups that form relatively strong hydrogen bonds with the hydroxyl groups of both the DA and EC, and the other is the carbonyl groups that form relatively weak hydrogen bonds with the ether groups of the EC. The IR band at $\nu = 1710\,cm^{-1}$ might be due to the stretching mode of the strong hydrogen-bonding carbonyl groups, and that at $\nu = 1735\,cm^{-1}$ might be due to the stretching mode of the weak hydrogen-bonding carbonyl groups. The above results suggest that the DA molecules in the EC-DA are relatively well distributed in the EC polymer matrix, and the DA molecules have relatively low chances to form hydrogen bonds with other DA molecules. Thus, the interactions between the EC polymer chains become weaker significantly as the DA molecules reside in the EC matrix, in which the DA acts as effective plasticizer. De Brabander et al. (2002) and Taylor and Zografi (1997) also observed similar results that the IR bands for the carbonyl stretching mode shifted due to the decrease or absence of the cyclic dimerization of acid functional groups in polymer dispersions.

3.3. Thermogravimetric properties

Fig. 6 shows the weight percentage of the DOP, DA and DA-C_n as a function of temperature. It is clear that the DA and DA-C_n are thermally more stable than the DOP. For example, the 5% weight loss temperature ($T_{d\text{-}5\%}$) of the DOP is ca. 198 °C, while those of the DA and DA-C_n are in the range of 267–294 °C (see Table 1). This indicates that if one used the DA and DA-C_n as the additives for the polymer processing, one could set the maxium temperature for the processing much higher temperatures, compared to that for the polymers containing DOP. In addition, it is seen that the weight % of the DA and DA-C_n decreases slowly up to ca. 300 °C and then

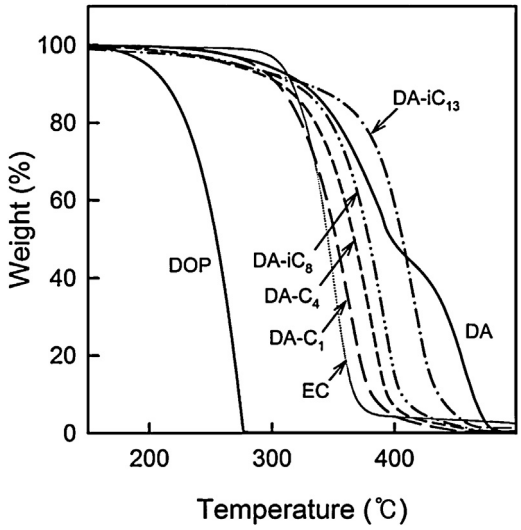

Fig. 6. Thermogravimetric curves of DOP, DA, DA-C_n, and EC as a function of temperature.

strongly. It is also found that the weight % curve shifts to high temperatures with increasing alkyl chain length, n, from 1 to 13. At this point, it should be mentioned that the weight % of the EC seems to remain constant up to 300 °C, and decreases drastically, and the $T_{d\text{-}5\%}$ of the EC is 307 °C that is not much different from the value reported elsewhere (Li, Huang, & Bai, 1999). The TGA data shown in Fig. 6 indicate that the thermal stability of the DA-C_n might be, at least, comparable to or even better than that of the EC. Also, it should be noted that the DA seems to go through two decomposition mechanisms, compared to just one mechanism for the rest. However, the investigation on the two decomposition mechanisms is beyond the scope of this work, and, thus, we do not discuss it any more here.

Fig. 7(a) shows the weight percentage of EC and EC composites containing 30 phr of DOP, DA or DA-C_1. The thermal decomposition of EC begins at ca. 300 °C and is completed at ca. 390 °C. On the other hand, the weight loss of the EC-DOP composite starts at ca. 200 °C, which is due to the presence of thermally unstable DOP; other than that, the thermal decomposition behaviour of the EC-DOP is similar to the that of EC. In the cases of the EC-DA and EC-DA-C_1, major decompositions occur in the temperature range of ca. 320–380 °C, related with the thermal degradation of EC. It is also seen that above 380 °C, the wight percentages of EC containing DA or DA-C_1, being more thermally stable than DOP, are higher than those of EC and EC-DOP. These findings indicate that the DA derivatives can be used as additives that allow the EC matrix to maintain its thermal stability. Fig. 7(b) exhibits that, as expected, with increasing amount of DA the onset temperature of degradation shifts to low temperatures progressively. However, it should be noted that even the EC-DA(50) is thermally stable at 300 °C, implying the possbile applications of DA as polymer additives used at high temperatures.

3.4. Dynamic mechanical properties

We measured the dynamic mechanical properties of the EC containing varying amounts of DOP, DA or DA-C_n. Fig. 8 shows the storage moduli (E') and loss tangents of the EC-DA as a function of temperature. In the log E' vs. temperature plots, it is seen that the EC shows a glassy modulus up to ca. 130 °C, and goes through a glass transition (T_g) in the temperature range of ca. 130–160 °C, and exhibits a plateau at log E' (Pa) = ca. 7.4 up to ca. 200 °C. Above ca. 200 °C, the storage modulus of the EC starts to decrease drastically with increasing temperature, i.e. the EC begins to flow. At

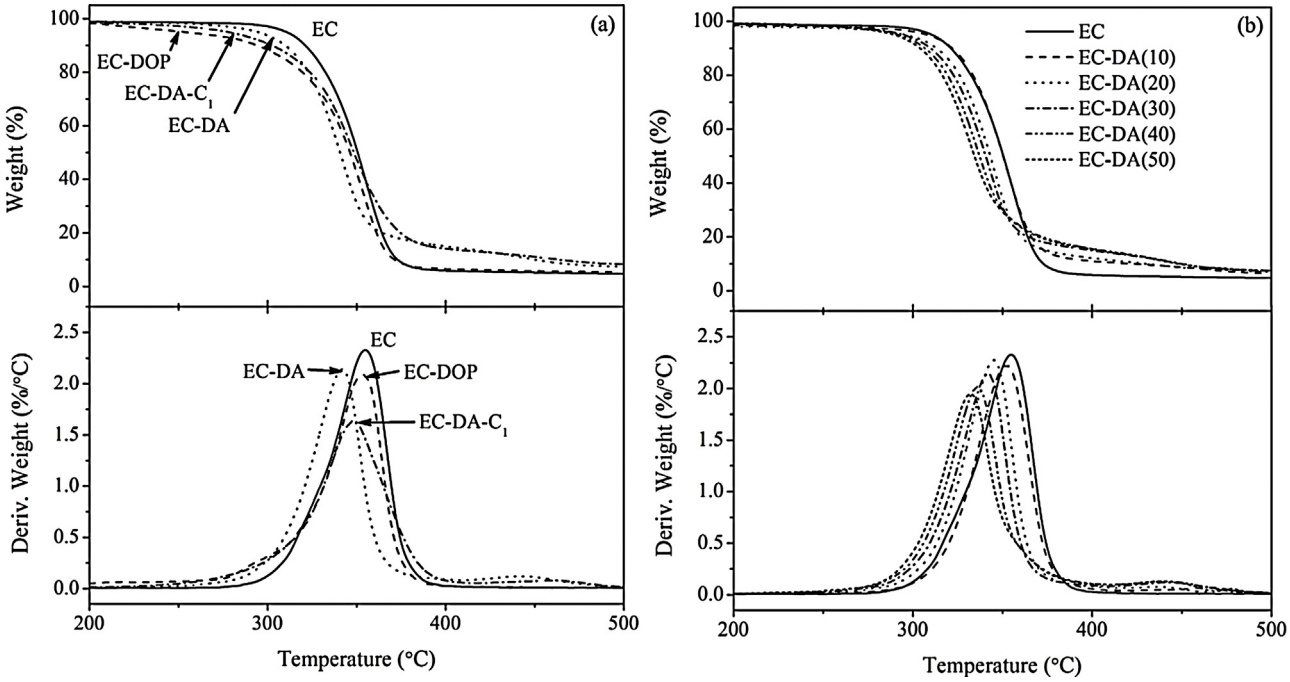

Fig. 7. (a) (top) Thermogravimetric and (bottom) differential thermogravimetric curves of EC containing 30 phr of DOP, DA, or DA-C_1 as a function of temperature. (b) (top) Thermogravimetric and (bottom) differential thermogravimetric curves of EC containing varying amounts of DA.

this point, it should be noted that the plateau modulus of the EC is much higher than the rubbery modulus of common polymers (e.g. log E' (Pa) < ca. 6.0). This is due to the presence of intermolecular interactions (i.e. hydrogen bonds) in the EC, as was mentioned before (Rekhi & Jambhekar, 1995; Gupta & Sahoo, 2001). It is known that this type of interactions could increase the rubbery modulus (Nielsen & Landel, 1994).

In the case of the EC-DA, the glassy modulus decreases slowly, and the slope of the curve for the transition becomes more gradual with increasing amount of the DA, which is due to the increase in the heterogeneity of polymer phase (Nielsen & Landel, 1994). In addition, the rubbery modulus decreases progressively, which will be discussed later in more detail, and shifts to lower temperatures, but the temperature range for the rubbery state increases. Loss tangent

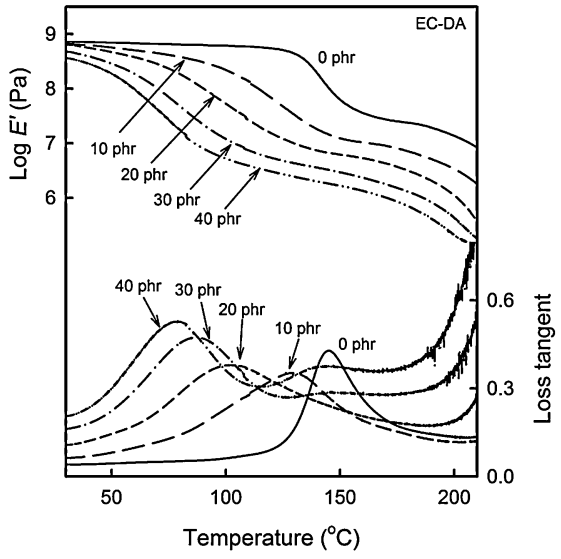

Fig. 8. Storage modulus (E') and loss tangent of the EC containing varying amounts of DA, measured at 1 Hz. The amount of DA in the sample is marked near each curve.

(tan δ) curves show that a single tan δ peak is seen for the EC at ca. 145 °C. Sakellariou, Rowe, and White (1986), Tarvainen et al. (2003), Crowley et al. (2004), and Lai. Pitt, and Craig (2010) also reported that the T_g of the EC determined by using differential scanning calorimetry (DSC) was in the range of ca. 120–130 °C. According to the fact that the T_g obtained by using the DSC (10 °C/min heating rate) was usually ca. 10–20 °C lower than that obtained by using the DMA (1 Hz data) (Kim, Wu, & Eisenberg, 1994), the tan δ peak at ca. 145 °C for the EC of the present work would be related with the glass transition. With increasing DA content, the tan δ peak shifts to lower temperatures, with increasing the peak width. Again, the broadening of the peak is assumed to be due to the increase in the heterogeneity of the polymer matrix phase (Nielsen & Landel, 1994). In the cases of the EC samples containing 30 or 40 phr of DA, they show an additional weak tan δ peak at ca. 140 °C that is close to the peak position of the pure EC. The other EC-C_n series also show similar results (data are not shown here).

For the comparison of the effects of the alkyl chain length of the DA-C_n on the dynamic mechanical properties of the EC-DA-C_n, the storage moduli (E') plots of the EC and EC containing 30 phr of DOP, DA, or DA-C_n as a function of temperature are shown in Fig. 9. It is seen that at room temperature the EC-DOP exhibits the lowest storage modulus, compared to the rest of samples. In addition, the EC-DOP shows the T_g in a temperature range of ca. 30–80 °C and a long descending plateau related to a rubbery modulus. Above ca. 150 °C, the sample starts to flow.

In the case of the EC-DA, the storage modulus value at ca. 30 °C is between those of the EC and EC-DOP. Interestingly, the modulus curve of the EC-DA looks similar to that of the EC-DOP, except for the differences in the onset temperatures of the sample flow. That is, the EC-DA begins to flow at 175 °C, but the EC-DOP starts to flow at ca. 150 °C. For the EC-DA-C_1, the onset temperature for the flow is ca. 160 °C, which is only 10 °C higher than that of the EC-DOP and ca. 15 °C lower than that of the EC-DA. The rest of the EC-DA-C_n samples show the shift of the modulus curve to high temperatures progressively with increasing alkyl chain length. However, the flow regions seem to merge into one point. In addition, it is seen that the temperature range of the descending plateau is either relatively

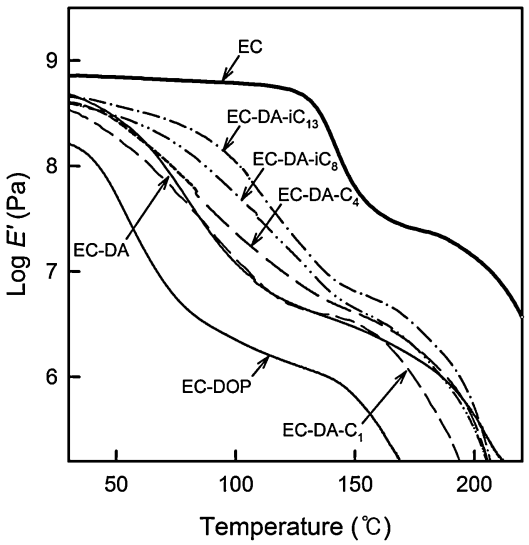

Fig. 9. Storage modulus (E') of the EC and EC containing 30 phr of DOP, DA, or DA-C_n as a function of temperature, measured at 1 Hz.

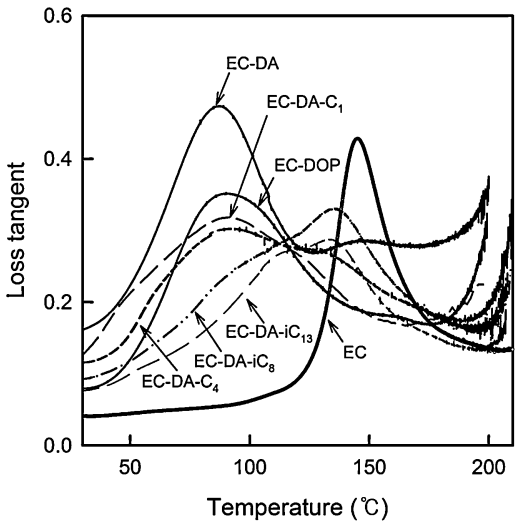

Fig. 11. Loss tangents of the EC and EC containing 30 phr of DOP, DA, or DA-C_n as a function of temperature, measured at 1 Hz.

short (e.g. ca. 30 °C) or relatively long (e.g. ca. 70 °C), depending on the samples. The above findings suggest that the DA or DA-C_n could be promising candidates that can be used instead of the DOP.

Shown in Fig. 10 are the moduli at the point of a minimum slope in the descending plateau segment of the log E' vs. temperature plots of EC-DOP, EC-DA and EC-C_n as a function of additive amounts. It is seen that the plateau moduli of the additive-containing EC decrease with increasing amount of additives. The plateau modulus data can be fitted with a first order polynomial. The equation for the straight line is as follows:

$$\text{Log}\,E' \quad (\text{Pa}) = 7.5 - 0.030w \quad \left(r^2 = 0.9924\right) \tag{2}$$

here w is the amount of the additives in phr, and r^2 is the linear least-squares correlation coefficient. It should be noted that the data at high concentrations of additives scatter, to some extent. This might be due to the fact that the increase in the additive concentration makes the samples too soft to be kept their dimensions for the DMA study at high temperatures where the samples exhibit their plateau moduli. This might cause the slightly scattering data at high additive concentrations.

Fig. 11 shows the loss tangents of the EC and EC containing 30 phr of DA or DA-C_n as a function of temperature. As mentioned before, the pure EC shows only one loss tangent peak at ca. 145 °C. On the other hand, a well-developed tan δ peak is seen for the EC-DOP at ca. 90 °C. For the EC-DA, a well-developed but relatively broad peak and a shoulder are present at ca. 80 °C and ca. 145 °C, respectively. In the case of the EC-DA-C_1, a very broad peak and a shoulder are seen at ca. 80 °C and ca. 125 °C, respectively.

At this point, it should be mentioned that some of the loss tangent curves seem to be a combination of two or three loss tangent peaks. Thus, we tried to de-convolute the peaks using a PeakFit software program (Systat Software, Inc.). Shown in Fig. 12 is one example of curve deconvolutions. The best fit curve for each of the samples can be obtained with an exponential background and Gaussian Areas for the peaks. The peak positions are the temperatures at the maxima of the low-temperature, middle-temperature, and high-temperature transition peaks. Present in Fig. 13(a) are the thermal transition temperatures obtained from the deconvolutions as a function of the amount of additives in the samples.

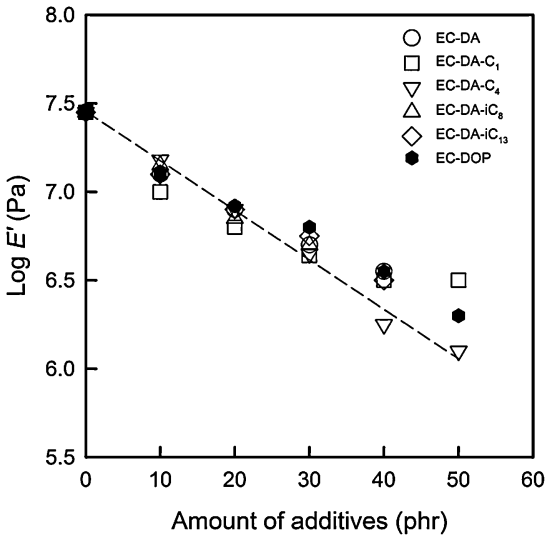

Fig. 10. Rubbery plateau of the EC-DOP, EC-DA and EC-DA-C_n as a function of amounts of additives, measured at 1 Hz.

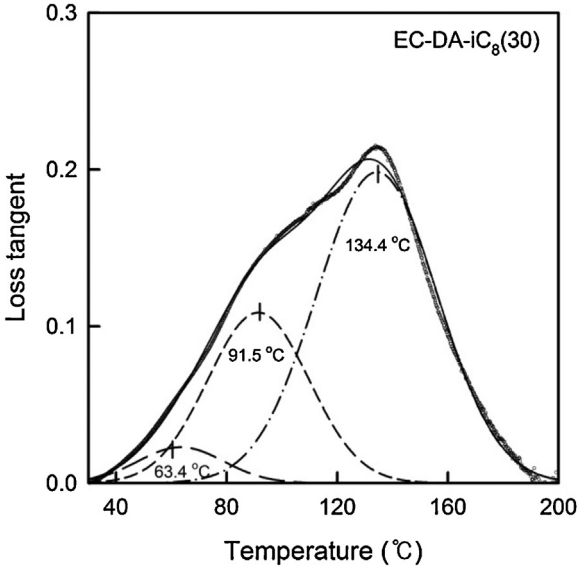

Fig. 12. Curve deconvolution results of EC-DA-iC_8(30).

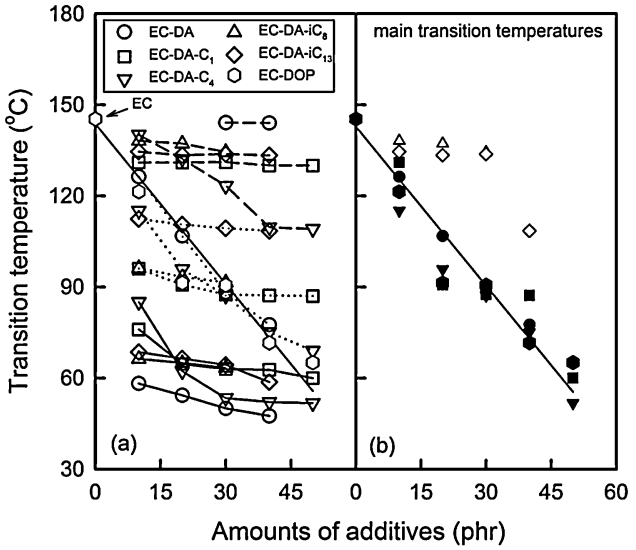

Fig. 13. (a) The thermal transition temperatures of the EC and EC containing varying amounts of DOP, DA, or DA-C_n as a function of the additive amounts, measured at 1 Hz. The straight solid line indicates the first order polynomial fitted to the data of EC-DOP. The dashed, dotted, and solid lines indicate the positions of the loss tangent peaks at high, middle, and low temperatures, respectively. (b) Filled symbols indicate the positions of the largest loss tangent peak among two or three de-convoluted peaks. The open symbols present the positions of the smaller loss tangent peaks. The straight solid line represents the first order polynomial fitted to the data of EC-DA, EC-DA-C_1, and EC-DA-C_4.

It is seen that two or three thermal transition temperatures are seen for the EC-DA and EC-DA-C_n samples. On the other hand, the EC-DOP samples show only one transition temperature that shifts to lower temperatures with increasing amount of the DOP. The data for the EC-DOP can be fitted with a first order polynomial. The equation for the straight line shown in Fig. 13(a) is as follows:

$$\text{Transition temperature } (^\circ\text{C}) = 144 - 1.76w \quad \left(r^2 = 0.9654\right) \quad (3)$$

The transition temperatures can be categorized into three temperature ranges; high temperature range (110–145 °C), middle temperature range (70–130 °C), and low temperature range (40–90 °C), depending on the type of the additives. The tan δ peak in the low temperature range might be involved in the disruption of the links between ester groups (Lizaso et al., 1999). It is also seen that the position of the peak of the EC-DA in the middle temperature range shifts to lower temperatures strongly with increasing additive amounts. Thus, it can be suggested that the peak might be involved in the glass transition of additive-rich phase. Lastly, the tan δ peak in the high temperature range is probably related with the glass transition of EC-rich phase. Fig. 13(b) shows the temperatures for the main transition as a function of the additive amounts. It is seen that the main transition peaks of the EC-DA, EC-DA-C_1 and EC-DA-C_4 shift to lower temperatures drastically as the additive amount increases, which is comparable to the peak shift of the EC-DOP (see Fig. 13(a)). In addition, when the amounts of additives are above 30 phr, the positions of the main peak of the EC-DA, EC-DA-C_1 and EC-DA-C_4 are close to that of the EC-DOP. It is clear that the transition temperatures for the EC-DA-iC_8 and EC-DA-iC_{13} do not change much, except for the EC-DA-iC_{13}(40). The rest of the data also can be fitted with a first order polynomial. The equation for the straight line shown in Fig. 13(b) is as follows:

$$\text{Transition temperature } (^\circ\text{C}) = 143 - 1.75w \quad \left(r^2 = 0.9573\right) \quad (4)$$

Interestingly enough, this equation is almost identical to Eq. (3) for the EC-DOP. The above results indicate that the DA, DA-C_1 and DA-C_4 in the EC can act as plasticizer like the DOP in the EC. In the case of the DA-iC_8 and DA-iC_{13}, they show poor miscibility with the EC, which might be due to their relatively low polarity. That is, the DOP has two alkyl chains, i.e. 2-ethylhexyl groups, but the DA has four alkyl chains, i.e. one hexyl chain, one octyl chain, and two heptyl chains. Thus, the increase in the alkyl chain length of the DA-C_n (see R_1 in Scheme 1) further induces the non-polarity significantly, and, thus, the DA-iC_8 and DA-iC_{13} might be less miscible with the EC. This suggests that the DA-iC_8 and DA-iC_{13} cannot behave like effective plasticizer like the DOP.

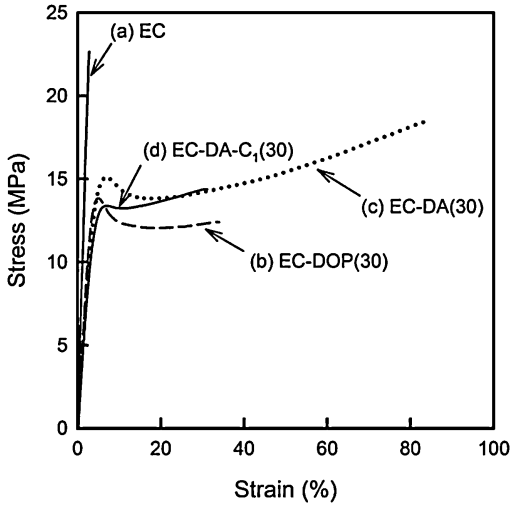

Fig. 14. Stress–strain curve and the Young's modulus of (a) EC, (b) EC-DOP(30), (c) EC-DA(30) and (d) EC-DA-C_1(30).

3.5. Tensile properties

The plasticization efficiency of the DA-C_n was also evaluated by using the tensile testing. The tensile stress and strain of the EC-DOP(30), EC-DA(30) or EC-DA-C_1(30) are compared in Fig. 14. From the tensile strength of the material, one can obtained the data on the mechanical resistance of the material due to the cohesion between the chains (Nielsen & Landel, 1994). On the other hand, the tensile strain at break gives us an idea on the material's plasticity that is related to the material's flexibility. The Young's modulus represents of the stiffness of an elastic material, which can be calculated from the initial stress/strain ratio. It is seen that the pure EC can be elongated only up to ca. 3% before failure, indicating its brittleness. However, the strain at break of the EC-DA(30) is found to be ca. 84%, which is more than twice that of the EC-DOP(30), keeping a little reduced stress at break, compared to that of the pure EC. The stress–strain properties of the EC-DA-C_1(30) are seen to be similar with those of the EC-DOP(30). The detailed data are listed in Table 3 that also includes the data for 50 phr samples. It is found that with increasing amount of the additives the stress at break and Young's moduli decrease. On the other hand, as the amount of the additives increases, the strains at break of the EC-DOP and EC-DA increase slowly, but that of the EC-DA-C_1 decreases. The most important

Table 3
Stress–strain data of EC, EC-DOP, EC-DA, and EC-DA-C_n.

Samples	Stress at break (MPa)	Strain at break (%)	Young's modulus (MPa)
EC	22 ± 2	3 ± 0.3	856 ± 84
EC-DOP(30)	12 ± 1	35 ± 9	456 ± 21
EC-DOP(50)	5 ± 0.5	46 ± 11	120 ± 14
EC-DA(30)	18 ± 1	84 ± 14	405 ± 20
EC-DA(50)	10 ± 1	87 ± 4	133 ± 15
EC-DA-C_1(30)	14 ± 0.4	32 ± 5	369 ± 52
EC-DA-C_1(50)	5 ± 0.6	15 ± 5	135 ± 19

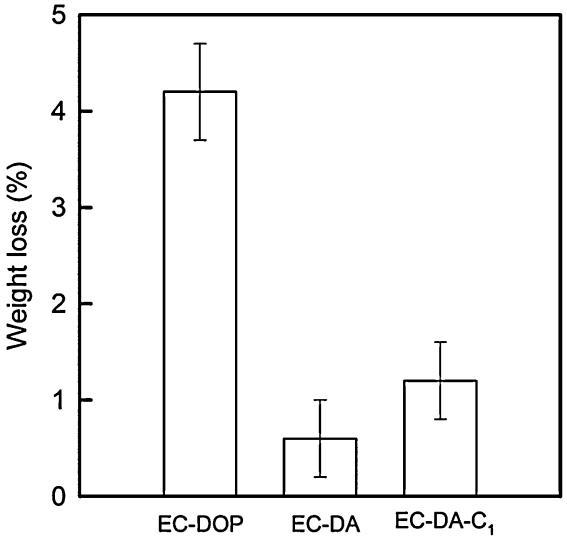

Fig. 15. Percentage of the weight loss of the EC films containing DOP, DA, or DA-C_1, extracted in deionized water for 24 h.

finding is that the EC-DA samples elongate more than any other samples. This is due to the presence of the DA in the EC. That is, as suggested in the section dealing with the IR data, the presence of the DA in the EC-DA leads to weaker interactions between the EC polymer chains, which results in the enhanced elongation of the EC.

3.6. Leaching test

The percentage of the weight loss of the EC films containing 30 phr of additives by extraction can be calculated as follows:

$$\text{Weight loss } (\%) = \frac{W_1 - W_2}{W_1} \times 100 \quad (4)$$

here W_1 and W_2 are the weight of film samples before and after the extraction, respectively; Fig. 15 shows the results.

It is known that the leaching of additives from polymer (i.e. plastics) is affected strongly by the strength of interactions between the polymer chains and additives (Lardjane & Belhaneche-Bensemra, 2009; Kastner, Cooper, Marić, Dodd, & Yargeau, 2012). Therefore, the strong hydrogen bonds between the hydroxyl groups of the EC and the acid groups of the DA can increase the resistance to leaching. In the present work, the phthalate plasticizer, DOP, is vulnerable to leaching, resulting in ca. 4.2% weight loss of the EC-DOP; this is similar to the value obtained by Crosthwaite, Muldoon, Dixon, Anderson, and Brennecke (2005). The EC-DA and EC-DA-C_1 samples show weak leachability (i.e. 0.6% and 1.2% weight loss, respectively). The results obtained from the leaching tests indicate that two acid functional groups of the DA play a significant role than the ester functional groups of the DOP and DA-C_1. Furthermore, the bulky structures and larger molecular weights (M_W) of the DA (M_W = 602.9) and DA-C_1 (M_W = 633.1) might be additional factors that reduce the leachability of the DA and DA-C_1, compared to the DOP (M_W = 390.6).

4. Conclusions

In this study, we synthesized DA containing a small amount of TA using the waste vegetable oil. Then, we converted them into their alkyl ester DA-C_n forms using an esterification reaction with proper alcohols. The DA and DA-C_n were found to be thermally more stable than the DOP. As the main part of our study, we prepared the EC films containing either DOP or DA or DA-C_n. We observed that the EC containing either DOP or DA or DA-C_n with short alkyl chains did not show phase separation in a micro-scale. We also found that the rubbery moduli of the EC were affected not by the type of the additives but by the amount of the additives. On the other hand, the main transition temperatures of the EC containing either DOP or DA or DA-C_1 or DA-C_4 decreased with increasing amounts of the additives, and the rates of decreasing transition temperatures were very similar to each other, implying that those additives could be used as effective plasticizer like the DOP. Furthermore, it was observed that the elongation at break of the EC-DA was better that those of the EC or EC-DOP or EC-DA-C_1, suggesting that the DA molecules, well-distributed in the EC matrix, weakened the interactions between the EC polymer chains. The results of the leaching test of the EC containing either DOP or DA or DA-C_1 revealed that the DA was released from the EC matrix more slowly than the DA-C_1, and the DOP was released faster. This means that the DA, if there were no problem caused by the acidity of the DA, might be better eco-friendly plasticizer than the DA-C_1, which, in turn, might be much better than the petroleum-based plasticizer, the DOP.

Acknowledgments

This study was supported by the R & D Center for Valuable Recycling (Global-Top Environmental Technology Development Program) funded by the Ministry of Environment, Korea (Project No. GT-11-C-01-270-0).

References

Bodmeier, R., & Paeratakul, O. (1994). Mechanical properties of dry and wet cellulosic and acrylic films prepared from aqueous colloidal polymer dispersions used in the coating of solid dosage forms. *Pharmaceutical Research*, *11*(6), 882–888.

Chen, G. Q., & Patel, M. K. (2012). Plastics derived from biological sources: Present and future: A technical and environmental review. *Chemical Reviews*, *112*(4), 2082–2099.

Crosthwaite, J. M., Muldoon, M. J., Dixon, J. K., Anderson, J. L., & Brennecke, J. F. (2005). Phase transition and decomposition temperatures, heat capacities and viscosities of pyridinium ionic liquids. *The Journal of Chemical Thermodynamics*, *37*(6), 559–568.

Crowley, M. M., Schroeder, B., Fredersdorf, A., Obara, S., Talarico, M., Kucera, S., et al. (2004). Physicochemical properties and mechanism of drug release from ethyl cellulose matrix tablets prepared by direct compression and hot-melt extrusion. *International Journal of Pharmaceutics*, *269*(2), 509–522.

De Brabander, C., Van den Mooter, G., Vervaet, C., & Remon, J. P. (2002). Characterization of ibuprofen as a nontraditional plasticizer of ethyl cellulose. *Journal of Pharmaceutical Sciences*, *91*(7), 1678–1685.

Fan, X. D., Deng, Y., Waterhouse, J., & Pfromm, P. (1998). Synthsis and characterization of polyamide resins from soy-based dimer acids and different amides. *Journal of Applied Polymer Science*, *68*(2), 305–314.

Gupta, K. C., & Sahoo, S. (2001). Graft copolymerization of acrylonitrile and ethyl methacrylate comonomers on cellulose using ceric ions. *Biomacromolecules*, *2*(1), 239–247.

Halden, R. U. (2010). Plastics and health risks. *Annual Review of Public Health*, *31*, 179–194.

Kastner, J., Cooper, D. G., Marić, M., Dodd, P., & Yargeau, V. (2012). Aqueous leaching of di-2-ethylhexyl phthalate and "green" plasticizers from poly(vinyl chloride). *Science of the Total Environment*, *432*, 357–364.

Kim, J.-S., Wu, G., & Eisenberg, A. (1994). Viscoelastic properties of poly(styrene-*co*-acrylate) and poly(vinylcyclohexane-*co*-acrylate) ionomers. *Macromolecules*, *27*(3), 814–824.

Krauskopf, L. G. (2003). How about alternatives to phthalate plasticizers? *Journal of Vinyl and Additive Technology*, *9*(4), 159–171.

Labrecque, L. V., Kumar, R. A., Davé, V., Gross, R. A., & McCarthy, S. P. (1997). Citrate esters as plasticizers for poly(lactic acid). *Journal of Applied Polymer Science*, *66*(8), 1507–1513.

Lai, H. L., Pitt, K., & Craig, D. Q. M. (2010). Characterization of the thermal properties of ethylcellulose using differential scanning and quasi-isothermal calorimetric approaches. *International Journal of Pharmaceutics*, *386*(1–2), 178–184.

Lardjane, N., & Belhaneche-Bensemra, N. (2009). Migration of additives in simulated landfills and soil burial degradation of plasticized PVC. *Journal of Applied Polymer Science*, *111*(1), 525–531.

Lee, S., Kim, Y. W., Yoo, S. H., Kim, N. K., Shin, J., & Yoon, B. T. (2013). Synthesis and lubricating properties of dimer acid derivatives based on used vegetable oil. *Applied Chemical Engineering*, *24*(5), 530–536.

Li, X.-G., Huang, M.-R., & Bai, H. (1999). Thermal decomposition of cellulose ethers. *Journal of Applied Polymer Science*, *73*(14), 2927–2936.

Lizaso, E., Muñoz, M. E., & Santamaría, A. (1999). Formation of gels in ethylcellulose solutions. An interpretation from dynamic viscoelastic results. *Macromolecules*, *32*(6), 1883–1889.

Luckachan, G. E., & Pillai, C. K. S. (2011). Biodegradable polymers—A review on recent trends and emerging perspectives. *Journal of Polymers and the Environment*, *19*(3), 637–676.

Lunt, J. (1998). Large-scale production, properties and commercial applications of polylactic acid polymers. *Polymer Degradation and Stability*, *59*(1–3), 145–152.

Nielsen, L. E., & Landel, R. F. (1994). *Mechanical properties of polymers and composites* (2nd ed.). New York, NY: Marcel Dekker, Inc.

Paschke, R. F., Peterson, L. E., & Wheeler, D. H. (1964). Dimer acid structures. The thermal dimer of methyl 10-*trans*, 12-*trans*, linoleate. *Journal of the American Oil Chemists' Society*, *41*(11), 723–727.

Peña, J. R., Hidalgo, M., & Mijangos, C. (2000). Plastification of poly(vinyl chloride) by polymer blending. *Journal of Applied Polymer Science*, *75*(10), 1303–1312.

Qin, Y., & Wang, X. H. (2010). Carbon dioxide-based copolymers: Environmental benefits of PPC, an industrially viable catalyst. *Biotechnology Journal*, *5*(11), 1164–1180.

Rahman, M., & Brazel, C. S. (2004). The plasticizer market: An assessment of traditional plasticizers and research trends to meet new challenges. *Progress in Polymer Science*, *29*(12), 1223–1248.

Rekhi, G. S., & Jambhekar, S. S. (1995). Ethylcellulose—A polymer review. *Drug Development and Industrial Pharmacy*, *21*(1), 61–77.

Rem, P. C., Olsen, S., Welink, J. H., & Fraunholcz, N. (2009). Carbon dioxide emission associated with the production of plastics—A comparison of production from crude oil and recycling for the Dutch case. *Environmental Engineering and Management Journal*, *8*(4), 973–980.

Sakellariou, P., Rowe, R. C., & White, E. F. T. (1986). Polymer/polymer interaction in blends of ethyl cellulose with both cellulose derivatives and polyethylene glycol 6000. *International Journal of Pharmaceutics*, *34*(1–2), 93–103.

Tarvainen, M., Sutinen, R., Peltonen, S., Tiihonen, P., & Paronen, P. (2002). Starch acetate—A novel film-forming polymer for pharmaceutical coatings. *Journal of Pharmaceutical Sciences*, *91*(1), 282–289.

Tarvainen, M., Sutinen, R., Peltonen, S., Mikkonen, H., Maunus, J., Vähä-Heikkilä, K., et al. (2003). Enhanced film-forming properties for ethyl cellulose and starch acetate using *n*-alkenyl succinic anhydrides as novel plasticizers. *European Journal of Pharmaceutical Sciences*, *19*(5), 363–371.

Taylor, L. S., & Zografi, G. (1997). Spectroscopic characterization of interactions between PVP and indomethacin in amorphous molecular dispersions. *Pharmaceutical Research*, *14*(12), 1691–1698.

Wheele, D. H., & White, J. (1967). Dimer acid structures. The thermal dimer of normal linoleate, methyl 9-*cis*, 12-*cis* octadecadienoate. *Journal of the American Oil Chemists Society*, *44*(5), 298–302.